

## Radiative electron-hole recombination in a new sawtooth semiconductor superlattice grown by molecular-beam epitaxy

E. F. Schubert, Y. Horikoshi,\* and K. Ploog

Max-Planck-Institut für Festkörperforschung, D-7000 Stuttgart 80, Federal Republic of Germany

(Received 26 December 1984)

A new sawtooth-shaped conduction- and valence-band potential in GaAs is generated by alternating *n*- and *p*-type Dirac- $\delta$  doping, i.e., by interrupting growth of the GaAs host material but continuing doping. Photoluminescence measurements on this new superlattice at 2 and 77 K reveal high-intensity emission at energies below the band gap of the GaAs host material. The luminescence energy does *not* depend on the excitation density over five orders of magnitude. This result indicates short minority-carrier lifetimes even at low-density excitation and a stable low-energy band gap of the superlattice. The spontaneous carrier lifetime determined from high-intensity excitation amounts to 3.3 ns, which is comparable to bulk-type GaAs. The material design parameters for the new superlattice are established taking into account quantized electron and hole states in the V-shaped potential wells.

### I. INTRODUCTION

In 1969 Esaki and Tsu<sup>1</sup> proposed artificial semiconductor superlattices with the crystal potential modulated by a periodic variation of the doping concentration or of the composition. Free carriers propagating in the direction of the layer sequence experience the periodic superlattice potential in addition to the periodic potential of the host crystal. The dispersion relation and the energy bands are modified as compared to the host material. Compositional superlattices were realized by Chang *et al.*<sup>2</sup> and doping superlattices by Ploog *et al.*<sup>3</sup> using molecular-beam epitaxy (MBE). The interesting characteristics of conventional doping superlattices<sup>4-6</sup> are a tunable absorption coefficient and a tunable emission wavelength. The tunability originates from extremely long recombination lifetimes of photoexcited electrons and holes which are spatially separated by the modulated electric field of the doping superlattice. At high excitation intensities these electrons and holes screen the charge of ionized impurities, and a reduction of the original band-edge modulation results. This phenomenon makes the observation of *stimulated* emission at energies below the band gap difficult in conventional doping superlattices. The problem can be solved by realizing both short carrier lifetimes and a strong modulation of the band.

In the present approach, short lifetimes are achieved in a new type of superlattice which consists of periodic alternating *n*- and *p*-type Dirac- $\delta$  doped sheets separated by undoped material. We have recently produced doping profiles in GaAs equal to the Dirac- $\delta$  function by interrupting the crystal growth mode of the host material but evaporating the doping impurity during molecular-beam epitaxy.<sup>7,8</sup> A V-shaped potential well is generated by this doping profile and carriers occupy quantized energy levels due to the quantum size effect.<sup>9</sup> In this paper we present first low-temperature photoluminescence results and material design parameters for a new sawtooth superlattice in GaAs, built by alternating *n*- and *p*-type Dirac- $\delta$  doping.

The optical properties found in this superlattice differ from those observed in bulk-type material or in other superlattices.

### II. CONCEPT OF THE SAWTOOTH SUPERLATTICES

In the new sawtooth superlattice the doping atoms are localized within only one atomic monolayer of the GaAs host material. The doping profile  $N_D(z)$  is properly described by the Dirac- $\delta$  function:  $N_D(z) = N_D^{2D}\delta(z)$ ,

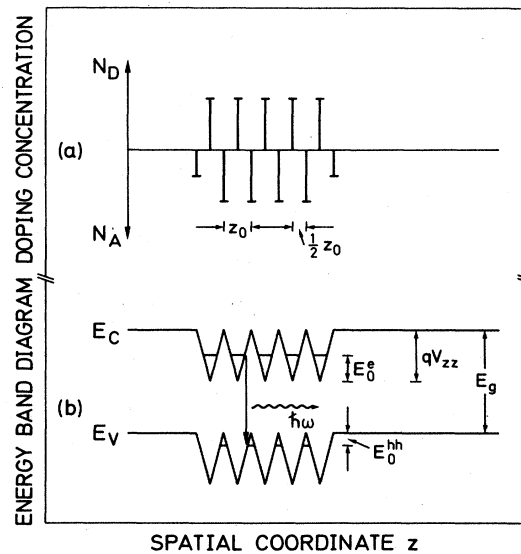


FIG. 1. (a) Doping profile of a sawtooth superlattice consisting of *n*- and *p*-type Dirac- $\delta$  doped layers with a period of  $z_0$ . (b) The sawtoothed-shaped conduction- and valence-band edges are caused by the charge of ionized donors and acceptors. The amplitude of the band modulation is  $qV_{zz}$ . The lowest electron and heavy-hole subband levels are  $E_0^e$  and  $E_0^{hh}$ , respectively. A quasiverbital radiative recombination in real space occurs between electron and hole subbands.

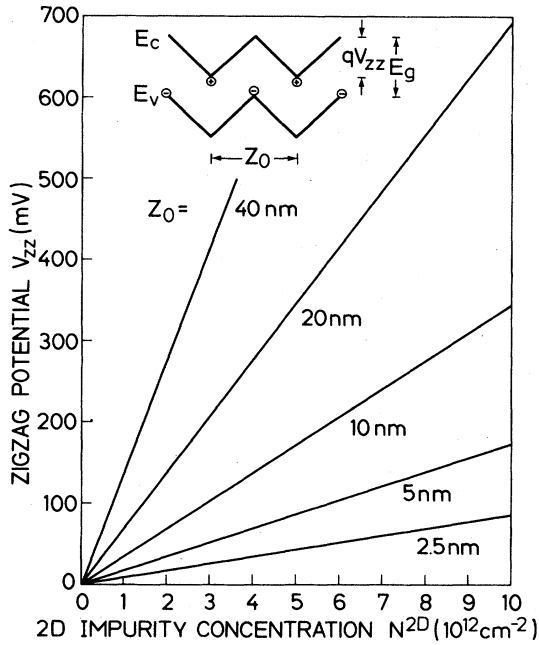


FIG. 2. Magnitude of the real-space energy-band modulation, called zigzag potential  $V_{zz}$ , as a function of the two-dimensional doping concentration  $N^{2D}$  for different superlattice periods  $z_0$ , as calculated from Eq. (1).

where  $N_D^{2D}$  is the two-dimensional (2D) doping concentration. In this study we employ alternating  $n$ - and  $p$ -type Dirac- $\delta$  doping with a concentration of  $2 \times 10^{12} \text{ cm}^{-2}$  carriers per sheet and a period of  $z_0 = 20 \text{ nm}$ . The doping profile is schematically shown in Fig. 1(a). Due to the proximity of donors and acceptors, electrons recombine with holes and a sawtooth-shaped conduction- and valence-band potential, as indicated in Fig. 1(b), is created. The amplitude of the sawtooth- or zigzag-shaped conduction band is given by the dopant density and the superlattice period (design parameters) of the crystal. The zigzag potential  $V_{zz}$ , which is depicted in the inset of Fig. 2, depends linearly on the superlattice period  $z_0$  and on the two-dimensional doping concentrations  $N^{2D}$  according to

$$V_{zz} = \frac{1}{4}(q/\epsilon)N^{2D}z_0, \quad (1)$$

where  $\epsilon$  is the permittivity of the semiconductor and  $q$  is the elementary charge. The amplitude of the zigzag potential obtained from Eq. (1) for different design parameters of the superlattice is shown in Fig. 2. The distance of the  $n$ - and  $p$ -type Dirac- $\delta$ -doped regions is taken as half the superlattice period  $z_0$  and the donor concentration  $N_D^{2D}$  is taken to be equal to the acceptor concentration  $N_A^{2D}$ .

In the narrow V-shaped potential well, size quantization occurs. The quantized energy levels are calculated by a method which we have recently applied to the triangular potential well of a selectively doped heterostructure.<sup>10</sup> The ground-state energy of the  $i$ th subband in a V-shaped potential well is given by

$$E_i = \frac{1}{4}2^{-1/3}(i+1)^{2/3} \left[ \frac{q^2 h N^{2D}}{\epsilon(m^*)^{1/2}} \right]^{2/3}, \quad i=0,1,\dots \quad (2)$$

where  $h$  is Planck's constant and  $m^*$  is the electron or heavy-hole effective mass, respectively. The calculated energies for the lowest and the first excited subbands are displayed in Fig. 3 as a function of doping density. Electrons have a higher subband energy  $E_0^e$  as compared to the heavy-hole subband energy  $E_0^{hh}$  due to the smaller effective mass of electrons. Radiative transitions occur from the lowest electronic subband of energy  $E_0^e$  to the lowest heavy-hole subband of energy  $E_0^{hh}$  in a *quasivertical mode* due to the proximity of electron and hole states. Consequently, the superlattice band gap  $E_g^{SL}$  is defined as

$$E_g^{SL} = E_g - qV_{zz} + E_0^e + E_0^{hh}. \quad (3)$$

Using this equation and the plots of the zigzag-potential (Fig. 2) and the subband energies (Fig. 3), we can tailor the real-space energy-band structure of the superlattice. The superlattice band-gap energy  $E_g^{SL}$  is smaller than the band-gap energy  $E_g$  of the host crystal for the parameters used in the present study. In principle, however, not only smaller superlattice band-gap energies but also larger superlattice band-gap energies as compared to the host GaAs crystal can be obtained by appropriate choice of the design parameters. For short superlattice periods  $z_0$ , at a given doping concentration in 2D, the zigzag potential decreases, but the subband energies remain constant. According to Eq. (3) the superlattice band-gap energy will consequently exceed the host band-gap energy  $E_g$ . This unique feature of the sawtooth superlattice needs further experimental and theoretical treatment and is not presented in the present paper.

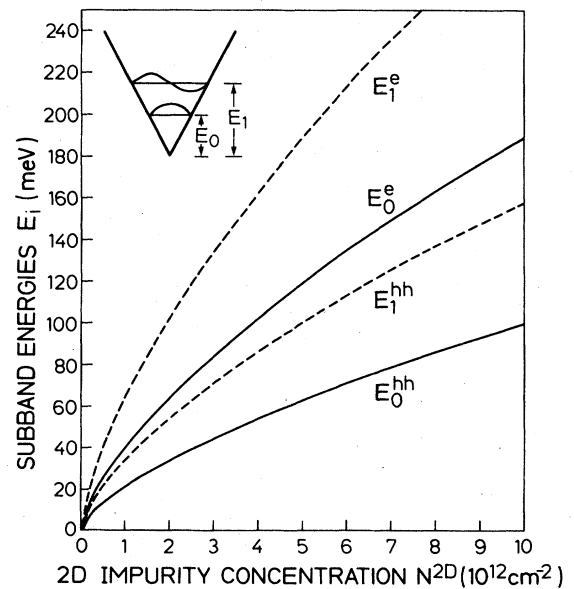


FIG. 3. Energies of the lowest and first excited electron and heavy-hole subband of the GaAs V-shaped potential well originating from a doping profile equal to the Dirac- $\delta$  function. The dependence of the subband energies on the doping density is obtained from Eq. (2).

In conventional GaAs doping superlattices, three-dimensional doping is used.<sup>1,3-6</sup> The maximum doping concentration thus depends on the solubility of the impurity element in the GaAs host material. A short superlattice period would result in a short carrier lifetime in conventional doping superlattices, but also in an undesired small band-edge modulation, because of the low doping density  $N_D(\frac{1}{2}z_0)$ . On the other hand, a large band-edge modulation can be achieved by enlarging the superlattice period which, however, implies long carrier lifetimes. Therefore, large band-edge modulations combined with short carrier lifetimes require the concept of Dirac- $\delta$  doping used in the new sawtooth superlattice.

When we prepare a conventional doping superlattice (no intrinsic regions) and a new sawtooth superlattice both having the same period  $z_0$  and the same amount of impurity atoms

$$N_D(\frac{1}{2}z_0) = N_A(\frac{1}{2}z_0) = N_D^{2D} = N_A^{2D}, \quad (4)$$

the zigzag potential of the sawtooth superlattice is

$$V_{zz} = \frac{1}{4}(q/\epsilon)N_D^{2D}z_0. \quad (5)$$

The modulation of the conventional doping superlattice is given by

$$V = \frac{1}{16}(q/\epsilon)N_Dz_0^2 \\ = \frac{1}{8}(q/\epsilon)N_D^{2D}z_0. \quad (6)$$

Comparison of Eqs. (5) and (6) demonstrates that the modulation of the sawtooth superlattice is two times larger, even if the same amount of impurity atoms and the same period is used in both types of superlattices. The modulation in sawtooth superlattices can even exceed a factor of 2, because the 2D impurity concentration is not limited by the solubility of the impurity element. Thus the large modulation in sawtooth superlattices makes possible very short superlattice periods.

### III. EXPERIMENTAL

The GaAs sawtooth superlattice samples are grown by molecular beam epitaxy on [100]-oriented semi-insulating GaAs substrates mounted on a continuously rotating substrate holder. Using a growth rate of  $1 \mu\text{m/h}$  and a growth temperature of  $550^\circ\text{C}$ , the residual impurity concentration of nominally undoped GaAs layers is  $p$ -type in the low  $10^{14} \text{ cm}^{-3}$  range. The Dirac- $\delta$ -function-like Si and Be doping profiles are achieved by interrupting the growth of the GaAs host material by closing the Ga shutter and leaving the As shutter open. The As-stabilized surface reconstruction is thus maintained while the shutter of the respective dopant effusion cell is opened for several seconds, resulting in an *impurity-growth mode*. The two-dimensional doping concentrations chosen for the studied superlattices are  $N_{\text{Si}}^{2D} = N_{\text{Be}}^{2D} = 2 \times 10^{12} \text{ cm}^{-2}$ . Thus only a small fraction of the Ga sites within one monolayer are occupied by doping atoms. The alternating  $n$ - and  $p$ -doped monolayers are separated spatially by 10 nm of GaAs, i.e., the periodicity of the superlattice is  $z_0 = 20 \text{ nm}$ . In the ground state the superlattice is completely depleted of free carriers. The photoluminescence

measurements are performed with the sample at 2 and 77 K by using the 647.1-nm line of a  $\text{Kr}^+$ -ion laser for excitation. The excitation intensity is varied from  $1 \mu\text{W}$  to more than 200 mW at a spot size of  $300\text{-}\mu\text{m}$  diameter by using neutral density filters. The resulting luminescence signal is analyzed with a 3/4-m monochromator (SPEX Industries, Inc.) and determined by a GaAs cathode photomultiplier. Normalization of the luminescence spectra to the photoresponse of the GaAs photomultiplier does not show a significant change of the observed luminescence peak energy. Additional measurements using a cathode photomultiplier with an  $S-1$  response yield similar results except for a more pronounced long-wavelength tail of the spectra.

### IV. RESULTS AND DISCUSSION

In Fig. 4 we show photoluminescence spectra obtained from a representative GaAs sawtooth superlattice of 50

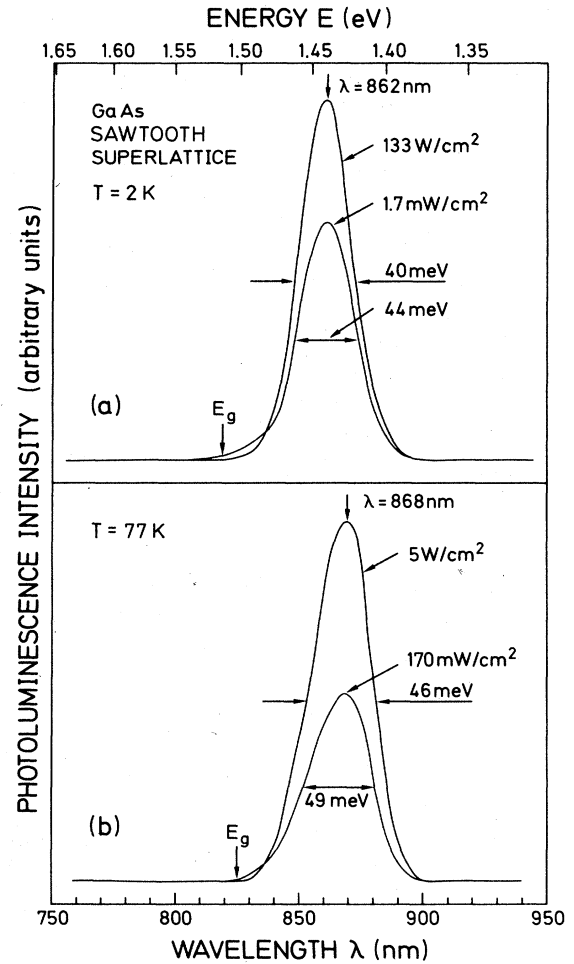


FIG. 4. Photoluminescence spectra obtained from a GaAs sawtooth superlattice ( $N^{2D} = 2 \times 10^{12} \text{ cm}^{-2}$ ,  $z_0 = 20 \text{ nm}$ , 50 periods) at 2 K (a) and 77 K (b) for different excitation densities using a GaAs cathode photomultiplier. The band-gap energy of bulk GaAs is marked by arrows. The observed luminescence peak energy is significantly lower than the band-gap energy of GaAs, and it does not change upon variation of the excitation intensity by more than four orders of magnitude.

20-nm periods using excitation densities of 1.7 mW/cm<sup>2</sup> and 133 W/cm<sup>2</sup> at 2 K [Fig. 4(a)] and 0.17 and 5 W/cm<sup>2</sup> at 77 K [Fig. 4(b)], respectively, and detection by a GaAs cathode photomultiplier. The band-gap energy of the host material is marked by an arrow. At the GaAs band-gap energy we observe no photoluminescence for all excitation intensities. This result indicates that only subband transitions and no band-to-band recombination of the GaAs host material contribute to the detected photoluminescence. It is important to note that the photoluminescence peak wavelength does not depend on the excitation intensity. In addition, the observed peak wavelength coincides with the value calculated from the superlattice design parameters by means of Eqs. (1)–(3). This means that the luminescence energy of the sawtooth superlattice can be preselected by proper choice of the design parameters but it cannot be *tuned* by changing the excitation conditions. The properties of sawtooth superlattices are thus in marked contrast to the features of conventional *n-i-p-i* crystals,<sup>6</sup> and provide significant advantages for practical application of the superlattice. The luminescence intensity obtained from the sawtooth superlattice is very high and comparable to that of bulk-type GaAs. The origin of the high intensity of radiative transitions is twofold. *First*, the spontaneous lifetime is fairly short due to quasivertical recombination and, as we will show later, comparable to that in bulk-type GaAs. *Second*, the luminescence transitions occur in nominally undoped GaAs, several nanometers away from the doped regions of the crystal [see Fig. 1(b) for illustration]. The full width at half maximum of the photoluminescence line is 40 meV at 2 K and 46 meV at 77 K. This line broadening is most likely caused by statistical size fluctuations of the quantum well as proposed by Weisbuch *et al.*<sup>11</sup> for compositional superlattices. At a measuring temperature of 77 K the peak energy of the detected photoluminescence is again smaller than the GaAs band-gap energy at 77 K (Ref. 12) and does not shift with excitation intensity [Fig. 4(b)]. The larger linewidth measured at 77 K is caused by an increase of the thermal energy of the photoexcited carriers.

In Fig. 5 we show the dependence of the photoluminescence peak wavelength on the excitation intensity over more than five orders of magnitude. The excitation density is varied from 1.7 mW/cm<sup>2</sup> to 360 W/cm<sup>2</sup>. Starting at excitation densities of about 130 W/cm<sup>2</sup>, band filling occurs in the subbands so that the ionized impurities are screened and the luminescence energy increases. We will now use this result to estimate the radiative lifetime  $\tau$  of our sawtooth superlattice. Band filling occurs when the Fermi level touches the bottom of the lowest subband, i.e. when the free-carrier concentration in the 2D electron gas (2DEG) of one electronic subband,  $n_{2\text{DEG}}$ , is equal to the 2D effective density of states  $N_C^{2\text{D}} = [m^*/(\pi\hbar^2)]k_B T$ , where  $k_B$  is the Boltzmann constant and the carrier temperature  $T$  is taken to be  $T = 50$  K. The radiative lifetime  $\tau$  of an electron is then obtained according to

$$\frac{dn_{2\text{DEG}}}{dt} = \frac{N_C^{2\text{D}}}{\tau} = \frac{P_1 z_0}{\hbar\omega_{\text{exc}} V_{\text{exc}}}, \quad (7)$$

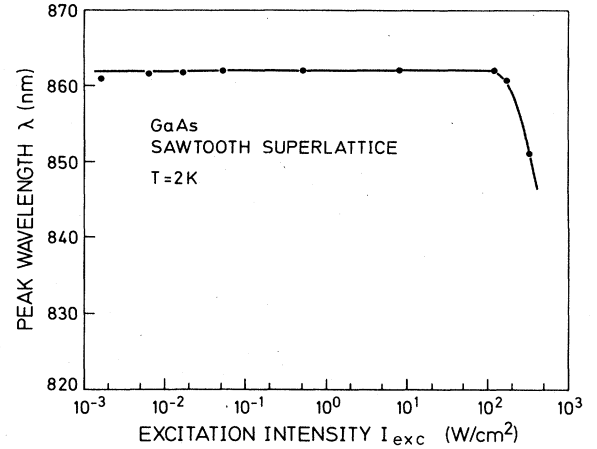


FIG. 5. Photoluminescence peak wavelength observed in a GaAs sawtooth superlattice at 2 K versus excitation density. The emission wavelength remains constant over five orders of magnitude of excitation-density variation. At about 130 W/cm<sup>2</sup>, band filling occurs and the ionized impurities are screened.

where  $P_1 \approx 100$  mW is the laser power at which the band filling occurs,  $\hbar\omega_{\text{exc}}$  is the photon energy of the exciting laser, and the excited volume  $V_{\text{exc}}$  is given by

$$V_{\text{exc}} = r^2 \pi (1/\alpha). \quad (8)$$

Here the radius of the laser spot is  $r = 150$   $\mu\text{m}$  and the absorption coefficient  $\alpha = 4 \times 10^4$  cm<sup>-1</sup>. Using Eqs. (7) and (8) we obtain a carrier lifetime of  $\tau = 3.3$  ns for the sawtooth superlattice. This short radiative lifetime is comparable to bulk-type GaAs. The short lifetime is probably caused by the enhanced radiative recombination due to the quasivertical transitions in real space. Therefore, nonradiative recombinations via midgap centers are unlikely. This result makes the sawtooth superlattice very promising for applications in photonic devices.

## V. CONCLUSION

We have presented the design rules of a new type of semiconductor superlattice which is obtained by alternating *n*- and *p*-type Dirac- $\delta$  doping of GaAs during molecular-beam epitaxial growth. The high-intensity photoluminescence spectra at 2 and 77 K exhibit emission wavelengths of 862 and 870 nm, corresponding to energies of 1.438 and 1.425 eV, respectively, which are significantly below the band gap of bulk-type GaAs. In contrast to conventional *n-i-p-i* crystals the luminescence peak wavelength does not depend on the excitation intensity over five orders of magnitude. The observed short carrier lifetime of 3.3 ns is due to a quasivertical type of recombination in real space. The present sawtooth superlattice exhibits a low-energy band gap which is stable even at high photoexcitation intensities. Using proper design parameters for this superlattice, we can also expect luminescence at energies higher than the band gap of the GaAs host material.

## ACKNOWLEDGMENTS

The authors would like to thank A. Fischer for expert help in sample preparation. The technical assistance of W. Heinz during the photoluminescence measurements is

gratefully acknowledged. Part of this work was sponsored by the Stiftung Volkswagenwerk and the Bundesministerium für Forschung und Technologie of the Federal Republic of Germany.

---

\*On leave from Nippon Telegraph & Telephone, Tokyo, Japan.

<sup>1</sup>L. Esaki and R. Tsu, IBM J. Res. Dev. **14**, 61 (1970).

<sup>2</sup>L. L. Chang, L. Esaki, W. E. Howard, and R. Ludeke, J. Vac. Sci. Technol. **10**, 11 (1973).

<sup>3</sup>K. Ploog, A. Fischer, and H. Künzel, J. Electrochem. Soc. **128**, 400 (1981).

<sup>4</sup>M. I. Ovsyannikov, Y. A. Romanov, V. N. Shabanov, and R. G. Loginova, Fiz. Tekh. Poluprovdn. **4**, 2225 (1970) [Sov. Phys.—Semicond. **4**, 1919 (1971)].

<sup>5</sup>G. H. Döhler, Phys. Status Solidi B **52**, 79 (1972).

<sup>6</sup>K. Ploog and G. H. Döhler, Adv. Phys. **32**, 285 (1983).

<sup>7</sup>H. P. Hjalmarson, J. Vac. Sci. Technol. **21**, 524 (1982).

<sup>8</sup>E. F. Schubert and K. Ploog (unpublished).

<sup>9</sup>A. Zrenner, H. Reisinger, F. Koch, and K. Ploog, in *Proceedings of the 17th International Conference on the Physics of Semiconductors, San Francisco, 1984*, edited by D. J. Chadi (Springer, New York, 1985).

<sup>10</sup>E. F. Schubert, A. Fischer, and K. Ploog, Phys. Rev. B **31**, 7937 (1985).

<sup>11</sup>C. Weisbuch, R. Dingle, A. C. Gossard, and W. Wiegman, Inst. Phys. Conf. Ser. **56**, 711 (1981).

<sup>12</sup>J. S. Blakemore, J. Appl. Phys. **53**, R123 (1982).